THE GAMMA-RAY SKY

L. Scarsi
Istituto di Fisica dell'Università, Palermo, Italy.

R. Buccheri, G. Gerardi, B. Sacco
Istituto di Fisica Cosmica e Tecnologie Relative CNR-Palermo

1. INTRODUCTION.

When we talk of Gamma-Ray Astronomy we refer in general to celestial photons covering the energy domain from a fraction of MeV up to the highest detected energies at hundreds or thousands of GeV. The six to seven decades altogether spanning the overall energy range constitute a very wide domain to be compared with those of the optical (less than one decade) or of the neighbouring X-Ray Astronomy (about two decades). The observational technique varies widely with changing energy; detector performances and characteristic parameters are not, in general, comparable. All of this has inevitably introduced, for the Gamma-Ray field, an additional subdivision in at least three sub-sectors:

Low and Medium Energy   :   0.1 to 20-30 MeV.
Intermediate and High Energy: 30 MeV to 5-10 GeV.
Very High Energy   :   the region beyond.

We will devote this review essentially to the High Energy sector; the choice stems from the fact that for these energies the observational situation has reached a rather advanced status with the Satellite SAS-2 and especially with COS-B which is still operational as of today. For the other two sectors the situation is moving slowly. The potential interest, specifically on the low energy side, is enormous; it is enough to recall the search for nuclear lines and the fact of looking for a connecting bridge between the typical X and Gamma-Ray Skies which look so different. On the other hand life is hard because of technical difficulties connected mainly with problems of background: HEAO 1, for example, has been rather disappointing with respect to expectation. On the "Very High Energy" side the problems derive mainly from the extremely weak signals to look for.

2. THE 30-5000 MeV ENERGY BAND

The Gamma-Ray Sky is best known in this energy range for which the exploration started some 20 years ago with a sizeable effort in balloon and satellite experiments, following a "call for attention" from theorists going as far back as 1952 (1-3).

2.1. Experiments before COS-B

Balloons, although limited by the interference of the atmospheric background and by reduced exposure time, succeeded in discovering the gamma-ray emission above 50 MeV from the Crab Nebula and its 33msec pulsar, the Vela Pulsar, the Galactic Center and the Cygnus regions, together with the diffuse emission at all galactic latitudes. As an example see the following references (4-8).

The satellite programme has listed a series of major missions with two of them (SAS-2 and COS-B) involving the full spacecraft capacity. We recall here the main chapters and major advancements; at the end the full story, as far as we know today, is that told by COS-B, the last experiment in the row.

Explorer XI, launched in 1961, carried on board a Gamma-ray experiment of the Group of MIT (9) and represented also the first space venture in High Energy Astrophysics; in its lifetime the experiment collected 31 gamma rays, but it failed in producing the evidence of their cosmic origin.

A clear evidence of galactic gamma-ray emission at $E_\gamma > 100$ MeV was first given by OSO-3 in 1968, again with an experiment of the Group of MIT (10); the gamma-ray telescope detected, within its rough angular resolution, a "line source" associated with the galactic disc, with a broad maximum in the inner Galaxy ($300° < \ell^{II} < 60°$), superimposed on a diffuse flux interesting all galactic latitudes. No localized sources were found and this can be explained, as we understand today, as due to the observational limits of the experiment. The interpretation put forward by Kraushaar et al. was of a galactic diffuse gamma-ray emission produced as a consequence (π° decay) of the interaction of cosmic ray particles with the diffuse interstellar matter; the high latitude emission was attributed to an extragalactic origin. The model, which fitted the observational data within a factor much better that an order of magnitude (quite satisfactory at the time, taking into account the level of incertitude for the parameters involved), was on the "economy" side, calling in only the most conventional factors and reducing to the minimum the role of any new assumption.

The third milestone has been SAS-2 of the NASA-Goddard Space Flight Center Group. The satellite operated between November 1972 and June 1973 and the experiment collected in its lifetime about 8000 gamma-ray
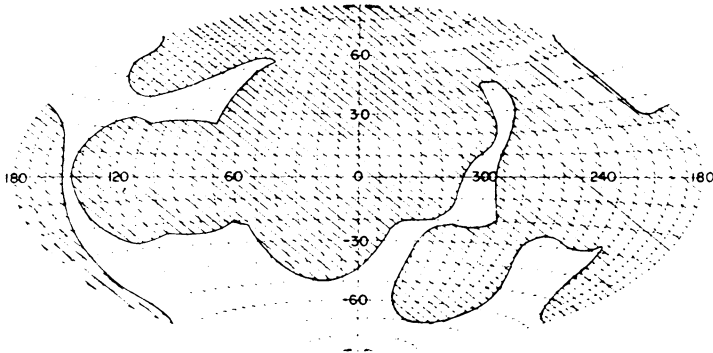
Fig. 1. Region of the celestial sphere viewed by SAS-2 (shaded area in
       the figure).

events above ∿35 MeV attributed to cosmic emission (11,12); the exposu-
re covered 60% of the celestial sphere (Fig. 1).
The Goddard Group has squeezed out of the data all possible information
and it has published recently the "very final" picture of the Gamma-ray
sky "as seen" by SAS-2. Ref. 13 contains in form of tables the details
of the analyzed gamma-ray data from the entire SAS-2 data base. Conclu-
sions on the "Galactic plane gamma-radiation" can be found in ref. 14,
15 and 16.
Most if not all of the SAS-2 reported results are overrided by the data
of COS-B which can count on much higher statistics collected during its
five years operation, a capability of measuring gamma-ray energies up
to several GeV, timing accuracy down to a fraction of millisecond in
absolute time, systematic and repeated observations of the various
regions of the sky. It is worthwhile however to present the SAS-2 re-
sults and conclusions with some detail for two main reasons:
a) They represent a coherent picture as given by a single experiment.
b) For some time to go the COS-B data will not be available both becau-
   se the experiment is still operating and because of the inherent,
   and by now well known viscosity of the Caravane Collaboration in
   releasing data (even more in interpreting them).

SAS-2: Localized galactic sources. The SAS-2 experimenters report the
observation of four localized sources along the galactic plane revealed
by a strong spatial enhancement coherent with the presence of a point-
like emitting object (14). The first two are the well known Crab Pulsar
PSR0531+21 and the Vela Pulsar PSR 0833-45. The third, γ 195+5 is con-
firmed by COS-B as CG 195+4; the 59 sec periodicity suggested by SAS-2

(17) and by COS-B in the first observation of the source (18) has not been any more confirmed by COS-B in successive observations. Because of the poor statistical significance of the data when a positive result was claimed, it seems clear that the presence of the periodicity should be considered doubtful and most probably the apparent result of random fluctuations. The fourth spatial enhancement has been identified (19) as due to Cygnus X-3, the identification being supported by the observation of the 4.8h periodicity characteristic at other wavelengths. COS-B does not confirm the existence of the 4.8h periodicity at the position of Cyg X-3 or for the nearest source found, CG 78+1 (20). These discrepancies put serious dubts on the source identification claimed by SAS-2. Also listed are two Radio Pulsars tentatively identified as gamma-ray sources (21): PSR 1818-04 and PSR 1747-46. The first one is not confirmed by COS-B; for the second the value of the period derivative $\dot{p}$ has been recently remeasured (22) and the value found (1.3×10^{-15} ss^{-1} instead of 70×10^{-15} ss^{-1}) would make the gamma flux claimed more than 100 times the rotational energy loss. We should consider therefore the effect observed for the two Radio Pulsars as most probably due to statistical random fluctuations.

In considering the distribution of gamma-rays in galactic longitude (binned in $\Delta \ell^{II} = 2.5°$) for $-10° \leqslant b^{II} \leqslant 10°$, Hartman et al. (14) report intensity peaks near the longitudes: 312°, 332°, 342° and 37°, which they consider associated with tangential directions to galactic spiral arm features.

SAS-2: Galactic plane gamma radiation. We report here directly the conclusions given by the SAS-2 Experimenter Group in their final paper(14).
- The large scale distribution of the gamma-ray flux (E $\gtrsim$ 35 MeV) from the Galactic Disc has several similarities to other tracers of galactic structure. The radiation is primarily confined to a thin disc, with off sets from $b^{II} = 0°$ similar to the "hat brim" feature revealed by radio-frequency measurements ($+2° \pm 0.5°$ for $90° < \ell^{II} < 175°$; $-2° \pm 0.5°$ for $205° < \ell^{II} < 250°$).
- The distribution in galactic latitude of the gamma-ray flux at different galactic longitudes suggests a local component for the broad distribution observed in directions away from the inner Galaxy and a predominant contribution from distant features ($\gtrsim$ 3 Kpc) for the narrower distribution observed toward the inner Galaxy.
- Enhancements are seen in the gamma-radiation in the galactic center and regions deduced from 21 cm measurements to be associated with spiral arms.
- Excluding the four strong localized sources, the energy spectrum of the gamma radiation seems to show no significant differences along the galactic plane. The overall spectral index (1.70 ± 0.14) is con-

sistent with the value (1.5 ± 0.3) deduced for the galactic component
at high latitudes ($|b^{II}| > 10°$).

By observing that:

the uniformity of the galactic gamma-ray energy spectrum, the smooth
decrease in intensity as a function of galactic latitude and the absen
ce of (SAS-2 observed) galactic sources at high galactic latitudes, all
argue in favour of a diffuse origin for the bulk of the galactic gamma-
radiation rather than a collection of localized sources

and on the assumption that:

cosmic-ray density be not uniform through the Galaxy but the density
in the plane be correlated with the matter density on the scale of ga-
lactic arms,

the SAS-2 group favours the conclusion that the majority of the obser-
ved gamma radiation above 35 MeV coming from the galactic plane seems
best explained in terms of diffuse emission with a cosmic-ray interac-
tion origin, the net contribution of localized sources, however, being
very uncertain primarily because of the limited angular resolution of
the telescope on board SAS-2.

SAS-2: Diffuse gamma-radiation away from the galactic plane. The data
from SAS-2 for the region of the sky corresponding to $10° < |b^{II}| < 90°$
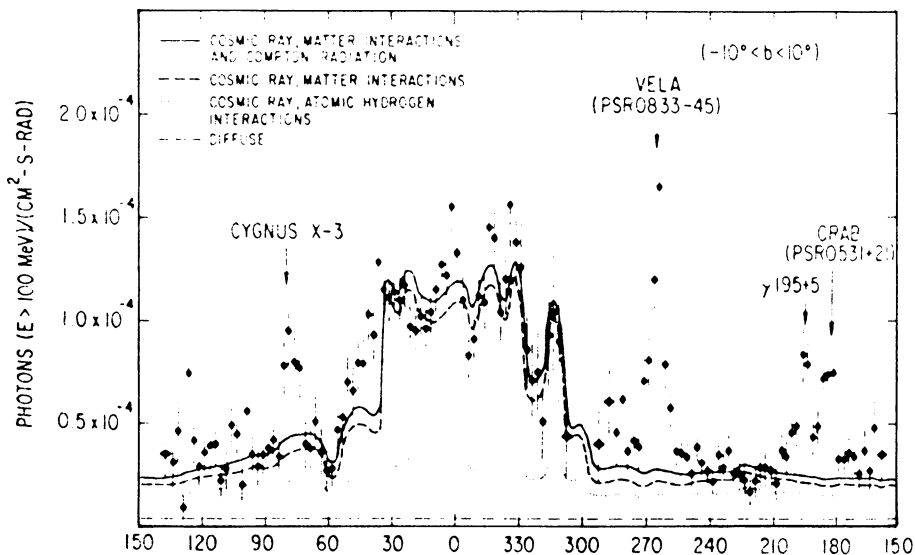
Fig. 2 (ref. 14). Gamma-ray flux (E ≥ 100 MeV) as a function of galactic
        longitude. The continuous lines show the comparison with the
        gamma-ray intensity predicted by the model of Kniffen et al.(23).

have confirmed the existence of a diffuse high galactic latitude gamma-radiation first reported by OSO-3. By considering the latitude, longitude and energy dependence of the gamma-ray flux revealed, the Goddard Group reaches the following conclusions (24-26):

- The diffuse gamma-radiation ($|b^{II}| > 10°$; $E \gtrsim 35$ MeV) consists of two components:

a) One considered to be a "galactic" component. It has the intensity strongly dependent on galactic latitude, joining smoothly to the intense regions of the plane; it is well correlated with the atomic hydrogen column density as deduced from the 21 cm measurements and the galactic synchrotron emission. The following are characteristic values:
spectral index (assuming a power law): 1.5 ± 0.3
intensity for galactic latitudes near the pole:
> 35 MeV : $(1.5 \pm 0.4) \times 10^{-5}$ photons/cm^2s sr.
>100 MeV : $(0.9 \pm 0.2) \times 10^{-5}$ "   "
intensity for a typical region with a galactic latitude of about $15°$:
> 35 MeV : $(6.9 \pm 1.7) \times 10^{-5}$ photons/cm^2s sr
>100 MeV : $(4.0 \pm 1.0) \times 10^{-5}$ "   "

b) One "isotropic", at least on a coarse scale, with galactic latitude. The following are the characteristic values:
spectral index (assuming a power law) : 2.7 (+0.4,-0.3)
intensity:
> 35 MeV $(5.7 \pm 1.3) \times 10^{-5}$ photons/cm^2s sr
>100 MeV $(1.0 \pm 0.4) \times 10^{-5}$ "   "
When extrapolated to 10 MeV with the values quoted above the power law joins smoothly to the "diffuse" isotropic intensity measured at low energies.

- No evidence is found of a cosmic ray halo surrounding the Galaxy in the shape of a sphere or oblate spheroid with galactic dimensions.

SAS-2: High galactic latitude localized sources. Extragalactic sources (27). SAS-2 does not report evidence for the existence of localized gamma-ray sources at high galactic latitudes. The experimenters list a set of upper limits for possible gamma-ray emission from active galaxies including those known to be X-ray emitters. The upper limits regard two energy regions: 35-100 MeV, and greater than 100 MeV. The values are spread over a rather wide range following differences in the diffuse emission level, the instrument exposure and the number of gamma-rays actually observed within the source region. The list includes a sample of Seyfert and N Galaxies, BL Lacertae objects, quasars, sharp emission line galaxies. The 95% confidence level limits for 35 -100 MeV expressed in keV/keV cm^2 s range from 1 to 10 (x 10^{-6}); the cor

responding values for E >100 Mev (expressed in photons/cm^2 s) range
from 0.5 to 5 (x 10^{-6}).

2.2. The "COS-B Gamma-Ray sky"

Until the second half of the years 1980's, i.e. until the
G.R.O. mission (the NASA Gamma Ray Observatory) will start to produce
some data after 1985, the gamma-ray sky in the 70-5000 MeV band will be
essentially that of COS-B, presumably with some adjustement for speci-
fic targets coming from dedicated balloons, or less probably Spacelab
experiments. Important results concerning the discrete sources are also
expected from the Franco-Russian satellite Gamma 1.
Before showing the COS-B data it is worthwhile introducing some basic
information on the satellite instrumentation, the mission profile, the
data analysis procedures and the data publishing policy of the Caravane
Collaboration. This with the purpose of an objective as possible presen
tation of the observational data, trying to explicitate the steps car-
ried out by the experimenters towards the interpretation and presenta -
tion of the results.

2.2.1. The COS-B Experiment

The general characteristics are described in ref. 28. The gam
ma-ray telescope is based on a magnetic-core wire-matrix Spark Chamber
triggered by a three element counter telescope. Beneath the telescope
is an energy calorimeter consisting of a CsI scintillator which absorbs
the secondary particles produced by the incident photons. Fig. 3 shows
the effective sensitive area, angular resolution and energy resolution
of the COS-B gamma-ray detector for axially incident gamma-rays satisfy
ing the selection criteria applied in the analysis. The angular resolu
tion is given as the FWHM of the spatial angular resolution or point-
-spread function, which best describes the experiment capability to
resolve two neighbouring point sources. It decreases asymptotically to
about 2° at high energies. The parameters described degrade with in -
creasing angle of incidence and the sensitive area falls to zero at an
angle of about 30°. Most of the results reported by the Caravane Colla-
boration are derived from measurements within 20° of the axis pointing
direction. Timing of gamma ray events is available with a final accura-
cy better than a fraction of millisecond in either the satellite or
the solar barycentre reference frame.
The COS-B experiment was designed, constructed and tested under the re-
sponsibility of a collaboration of research laboratories known as the
"Caravane Collaboration", whose members are listed in Table 1. The de-
finition of the observation programme and the analysis of the data are
also collaborative activities.
Data are analyzed independently in the various Laboratories of the Col
laboration, but they are jointly discussed in meetings and working ses-
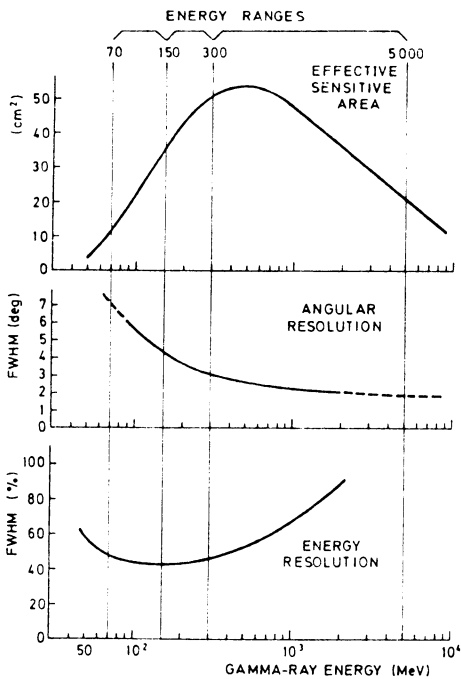
Fig. 3. Effective sensitive area, angular resoltution and energy resolution of the COS-B detector.

sions of a "Data Reduction Group" composed of representatives of each member Laboratory. Results are relea sed for publication only when a un- animous agreement is reached on the data treatement, elaboration and in- terpretation.This policy, while gua- ranteeing a maximum of objectiveness, has on the other hand the drawback of slowing down considerably the re- lease of results and of reducing the "Caravane Collaboration" published papers to bare straightforward pre- sentation of observational data with practically no comments and model interpretation reduced to an absolu- te minimum.

Launched on August 9, 1975 COS-B has operated since then with prac- tically unchanged performance; the instrument present status and the onboard consumable goods (gas for spark chamber flushing and gas for attitude control system) would per- mit an operational life at least until the end of •1981. At the moment, for budgetary reason, the COS-B operational life is assured only to september 1980. The orbital ele-

Table 1

THE CARAVANE COLLABORATION

Max-Plank-Institut für Physik and Astrophysik. Institut für Extraterre- strische Physik. Garching-bei-München.

Service d'Electronique Physique. Centre d'Etudes Nucleaires de Saclay.

Cosmic-Ray Working Group. Huygens Laboratory. Leiden.

Laboratorio di Fisica Cosmica e Tecnologie Relative CNR. Milano.

Laboratorio di Fisica Cosmica e Tecnologie Relative CNR. Istituto di Fisica Università di Palermo.

Space Science Department of ESA. ESTEC. Noordwijk.
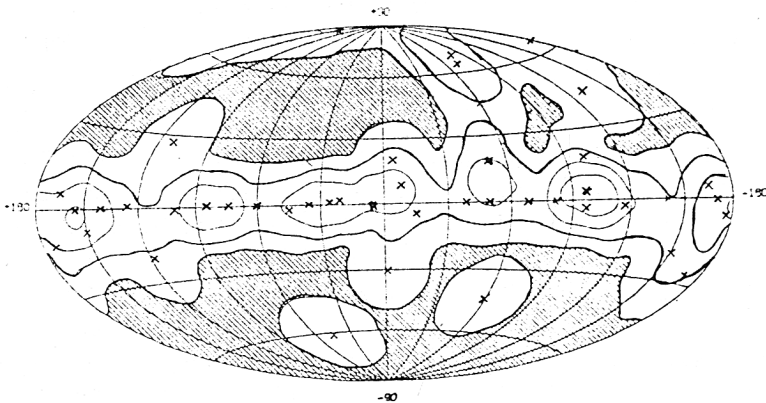
Fig. 4. Relative sky coverage between 17 August 1975 and 20 April 1980.
The unshaded area indicates the region of the sky observed
within 20° of the pointing direction (galactic coordinates).
The contour intervals are chosen to indicate the number of
times a given direction has been observed. Crosses indicate the
pointing directions.

ments at launch were: height of perigee = 340 Km; height of apogee =
= 99000 Km; inclination = 90.2 degree; drifted now (as for May 1980)
respectively to the values: 13.000 Km; 86.000 Km; 98°. The eccentric
orbit was chosen for scientific reasons (satellite for most of the ti-
me outside the radiation belts) and for technical reasons (for most of
the operational part of the orbit satellite in sight of an ESA ground
station).
The mission profile has been based on pointing to sky targets for
periods of four to five weeks. Presently is "on" the observation period
Nb.52 with the Cygnus region (ℓ^{II}=80°; b^{II}=0°) as a target.
Fig. 4 shows the relative sky coverage between launch and April 1980.
Two thirds of the observation time have been devoted to a systematic
scanning of the region of the galactic disc, with repeated or overlap-
ping observations (pointing direction $|b| < 10°$). The remaining third
has been addressed to high galactic latitudes, but with no claim to a
systematic coverage. The presence of a non-negligible gamma-ray instru
mental background induced by interaction of the Cosmic Radiation (non
modulated by the geomagnetic field) precludes the evaluation of a possi
ble diffuse isotropic component. This background has been reduced signi
ficantly with the progressing of the solar cycle.
        In the following paragraphs the main results obtained by COS-B
will be published.   In doing that, we will specify, case by case,
the "status" of the result reported: if fully and finally agreed by the

COS-B Data Reduction Group, it will be reported on behalf of the Cara-
vane Collaboration; if not yet at this stage, and therefore susceptible
of possibile modifications, the announcement engages only the responsa-
bility of the authors of this paper.

          2.2.2. The Large Scale Galactic Gamma-ray Emission
          The available data from COS-B constitute a complete high en-
ergy ($\gtrsim$ 70 MeV) gamma-ray survey of the Galactic disc. A first release
of the Sky-map of the Milky Way has been done by the Caravane Collabora
tion in December 1978 at the 9th Texas Symposium on Relativistic Astro-
physics (29); it referred to the satellite operation until February
1978 and covered the whole range of galactic longitudes. The data base
was constituted by 64.000 gamma-ray events collected during $\sim$700 days
corresponding to the 20 low $|b^{II}|$ out of 28 observation periods, lasting
$\sim$1 month each.An updated version covering the operation period up to
the end of 1979 and enlarging the data base to about 100.000 events is
presently under elaboration and it will be completed within the next
few months. Details of the analytical procedure can be found in (29).
The spark-chamber data are first analysed by an automatic pattern-reco
gnition programme to select likely gamma-ray events and subsequently
visually scanned in order to remove background and improve the direc-
tion determination. The events are then grouped in three energy bands
(70-150 MeV; 150-300 MeV and 300-5000 MeV; the band boundaries are
chosen to provide comparable statistical accuracy for each group of
events. Following the reconstructed direction of arrival, the events
are assigned to $0.5°$ x $0.5°$ bins; the resulting map is treated with a
smoothing procedure to obtain the best representation compatible with
the angular resolution of the gamma-ray telescope. The smoothing pro-
cedure chosen should not suppress the sharpest physically possible
peaks, without on the other hand reproducing peaks significantly narro-
wer than the point-spread function and therefore evidently produced by
statistical fluctuations.
Fig. 5 refers to the results obtained in the first analysis run (August
1975-February 1978) already published (29); the figure shows the longi
tude profiles in the three energy ranges. As it can be seen, more fine
structures are visible going from low energies to high energies in rela-
tion to the varying angular resolution of the telescope. Latitude profi
les have also been derived by these data and have been used to determi-
ne the intrinsic thickness of the emissivity taking into account the
instrument point-spread function. Fig. 6 shows an example together with
the unfolded angular thickness of the emitting region along the galac-
tic disc.
In Fig. 5 and Fig. 7 the intensity is given in "on axis" counts/s sr,
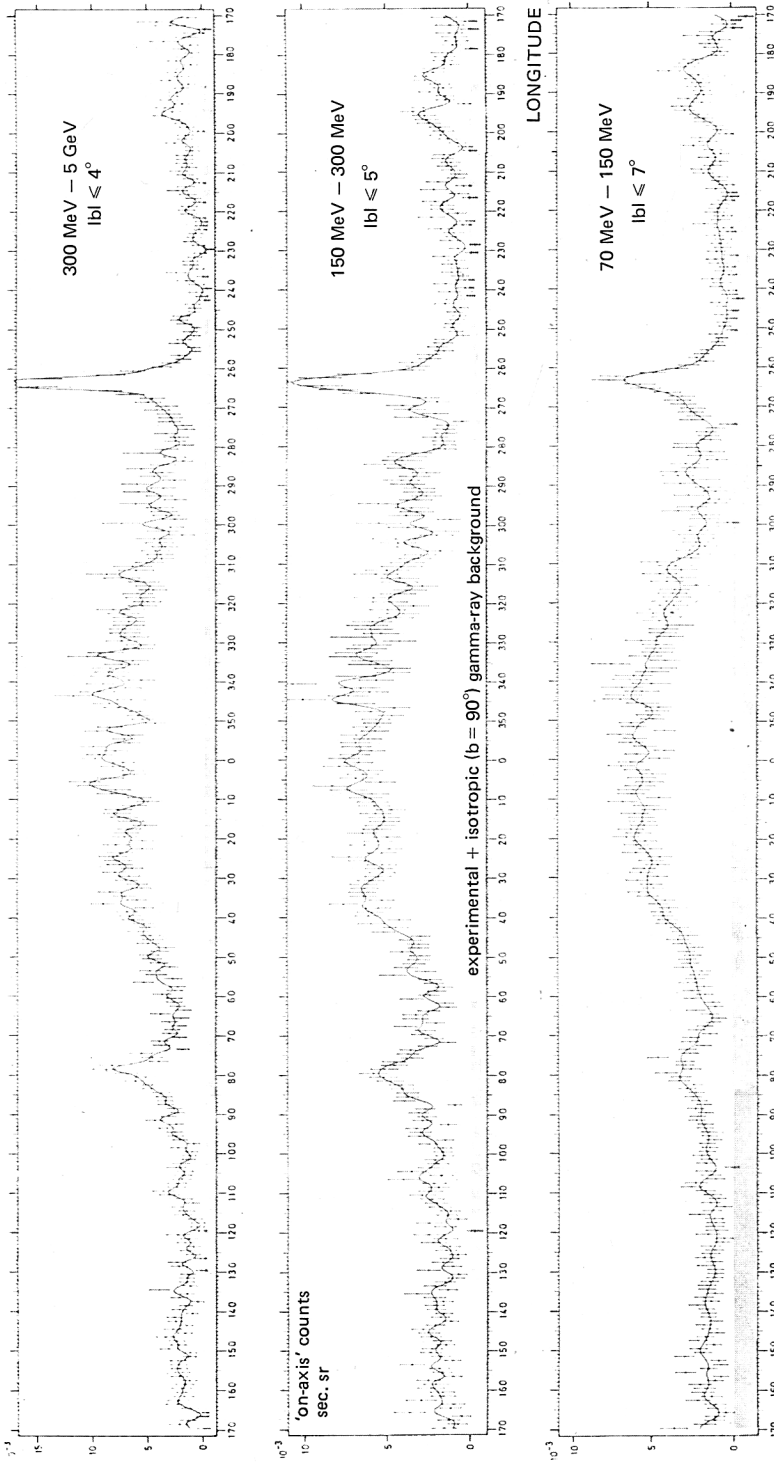
Fig.5. Longitude profiles of "on-axis" counts in three energy ranges.
The full line indicates the fitted surface.
The background is indicated by the shaded area.
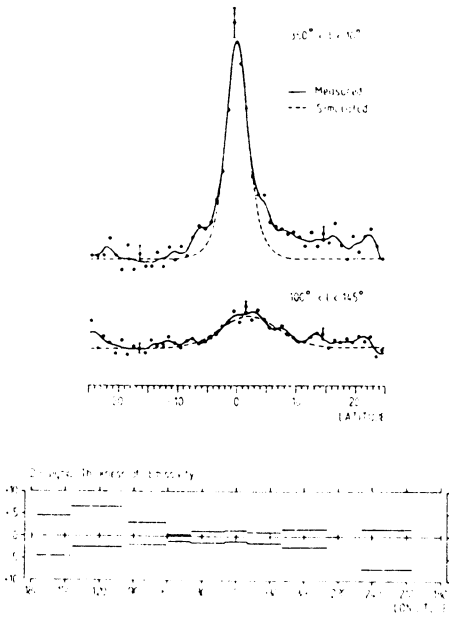
Fig. 6. Examples of latitude di-
stributions. Lower figure gives the
thickness of the gaussian distribu
tions describing the unfolded in-
trinsic emissivity at varying ga-
lactic longitudes.

which represent the number of gamma-
-ray events which would have been
recorded in the bin chosen if the ex
periment had been pointing there ob-
serving it "on axis". This presenta-
tion of the spatial distribution of
the photon arrival directions has
the advantage over the "photon flux"
maps of not being dominated by the
low energy component which is measu-
red with least accuracy in angular
resolution.

The definition of "photon flux" F_k
from a given sky bin k and the cor-
responding "on axis counts" are gi-
ven in Table 2.

Fig. 7 shows a map of the galactic
disc region, always seen by COS-B,
but derived on a data base 1.5 time
larger (corresponding to a compara-
tively longer observation time) than
that used in ref. 29.

This sky-map (courtesy of Dr. H.
Mayer-Hasselwander) is still preli-
minary, but it confirms substantially
the picture given in ref. 29, adding
some more detail.

Table 2

Definition of "photon flux" and of "on-axis counts" from a sky bin k of
angular size ω_k from which N_k gamma-ray events were recorded. E_i is
the energy of the event; θ_i is the incidence angle relative to the axis
of the experiment, T is the observation time; $\varepsilon(E)$ is the experiment's
effective area for axial incidence; $\eta(\theta_i, E_i)$ describes the decrease of
effective sensitive area with incidence angle.

$$F_k = \frac{1}{T\omega_k} \sum_{i=1,N_k} \frac{1}{\varepsilon(E_i)\,\eta(\theta_i,E_i)} \quad \text{photons cm}^{-2}\text{ s}^{-1}\text{ sr}^{-1}$$

$$G_k = \frac{1}{T\omega_k} \sum_{i=1,N_k} \frac{1}{\eta(\theta_i,E_i)} \quad \text{counts s}^{-1}\text{ sr}^{-1}$$
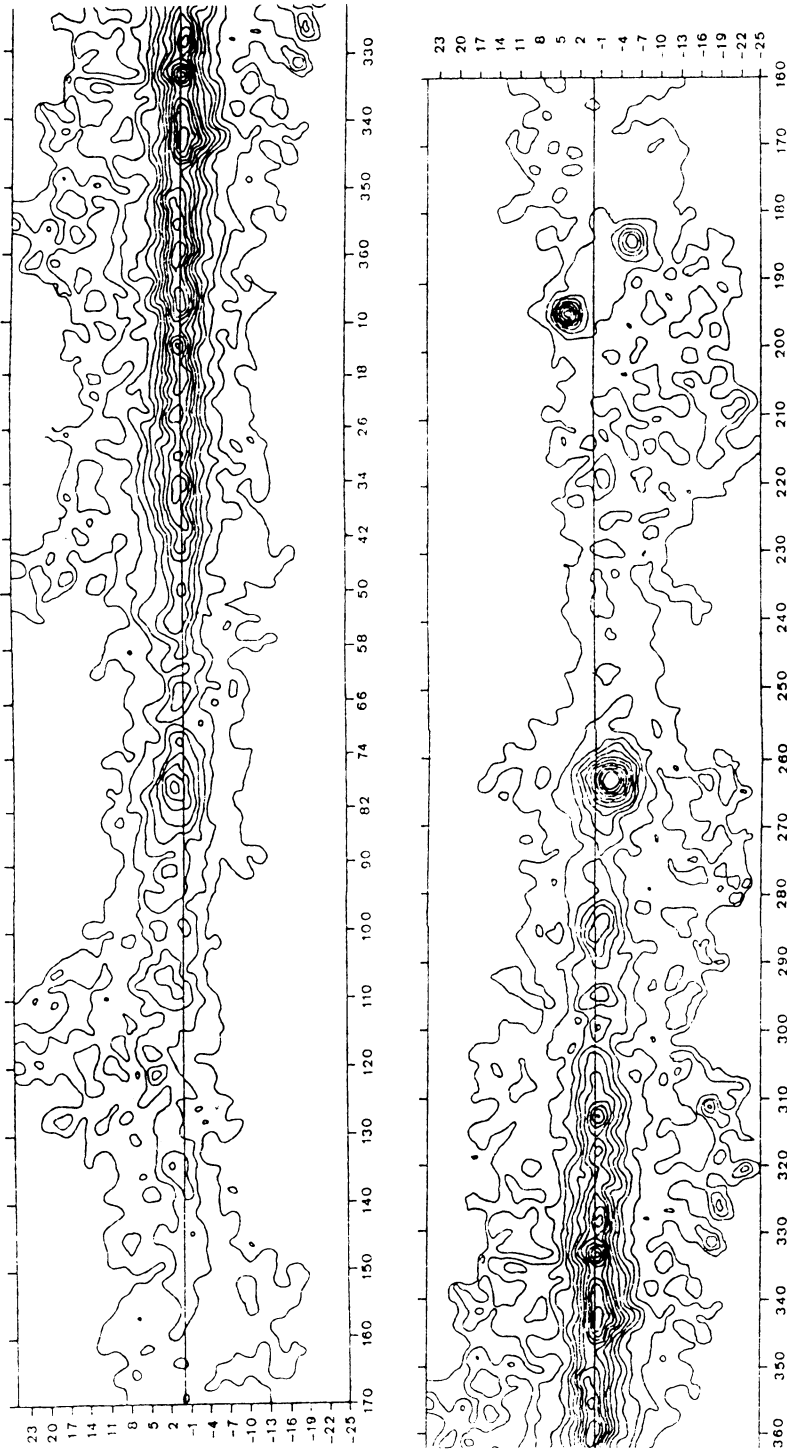
Fig. 7. Structure of the Galactic gamma-ray emission as measured by COS-B. Sky map of the Galactic Plane in the Energy Range 70 – 5000 MeV. The isointensity contour intervals represent "on-axis counts" s^{-1} sr^{-1} and are separated by 4×10^{-3}.

The observational data presented in the sky-map and the longitude, latitude profiles shown above give a projected picture of the Galaxy with no direct information of distances for the emitting regions (apart from those independently existing for the identified discrete sources).
A few basic points can be made:

a) The sky map taken along the galactic disc, even at a first rough inspection, shows the existence of several enhancements (localised excess counts) corresponding to the expected appearance for a point source; Vela and Crab, between others, are clear examples. By a systematic investigation with a cross-correlation procedure of the data with the point-spread function of the instrument (see paragraph 2.2.3.) numerous point-like sources have been evidenced. SAS-2 with an angular resolution comparable, if not better, to COS-B failed to recognize the importance of discrete sources most probably because of the limited statistics of the data base available for analysis. The discrete sources, following COS-B, can easily account for up to 50% of the total galactic emission; the pronounced granularity remaining in the maps after subtraction of the resolved sources suggests that possibly the 50% should be considered as a lower limit. The capability of detecting localized sources is conditioned by the limited angular resolution of the experiment against the background of the unresolved and diffuse galactic emission.

b) Strong and Worral (30) from the SAS-2 data, assuming a cylindrical symmetry, have estimated the absolute galactic luminosity above about 50 MeV: $L_\gamma \sim 5 \times 10^{38}$ erg/ s. This estimate is coherent with the COS-B data.

c) Taking latitude profiles as a function of longitude at high energies (>300 MeV) for which the angular resolution is better, the radiation appears to be confined to a thin disc. The peak of the excess has a small but significant latitude displacement from $b^{II}=0°$ corresponding to the "hat-brim" effect seen in the 21 cm line. The existence of two components in the disc emission first revealed by SAS-2 appears to be clearly established. A broad component appears at all galactic longitudes, with superimposed a narrow one for directions corresponding to the inner Galaxy ($55° < \ell^{II} < 285°$).The two components can be related to features at different distances in the Galaxy. By assuming a constant thickness of $\sim$ 200pc for the gamma-ray disc, the broader component can correlate well with local regions at $\lesssim$ 1 Kpc, while the narrow component appears to have its origin at a 3 to 6 Kpc distance and shows a strong variation with galactic longitude.

d) The wide component for the disc emission shows a broad excess at positive latitudes in the central region of the Galaxy and at negative

latitudes in the anticentre. Fichtel et al. (11) noticing a similar
behaviour in a qualitative analysis of the SAS-2 data suggested this
feature to be an indication of gamma-ray emission from the Gould
Belt of dust, gas and young stars at distances varying up to 450 pc
from the Sun. The gamma ray emission would derive from cosmic ray
(protons and electrons) interactions with the interstellar clouds
in the Belt (31-33). The discrete gamma-ray source of the COS-B ca-
talogue CG353+16 is positionally compatible with the ρ -Oph dark
cloud complex and its emission could be attributed to cosmic ray in-
teractions in the cloud (34). COS-B also reports the observation of
high-energy gamma-ray emission from the Orion cloud complex (37). In
general, without making a detailed correlation with individual
clouds and assuming a mass distribution for the Gould Belt as given
in ref. 35 and 36, with a production rate of gamma-rays of 2-3 x
x 10^{-25} photons ($\geqslant 100$ MeV) sec^{-1}, it is possible to justify appro-
ximatively the gamma-ray flux observed.

e) In considering the narrow galactic component, its longitude distribu
tion can be well correlated with many different galactic tracers and
it has been interpreted by several authors as implying the presence
of an enhanced flux of cosmic rays in the inner Galaxy. On the other
hand the presence of an important contribution from discrete sources
with an unknown integrated effect of the unresolved ones, together
with the arbitrary way in which several assumption can be made, ma-
kes the picture rather confuse.

2.2.3. Localised Gamma-ray Sources

One of the outstanding results of the COS-B mission is the com
pilation of a catalogue of discrete gamma-ray celestial sources. This
has produced a significant shift from the previous "way of thinking"
of the galactic emission as being substantially due only to diffuse
type processes. A first Catalogue of 13 objects in a survey covering
50% of the galactic plane has been published in 1977 (38), showing
their predominantly galactic nature. A new list of 29 has been successi
vely released by the Caravane Collaboration at the Erice Europhysics
Conference on Gamma-ray Astronomy (1979) and at the COSPAR Meeting at
Bangalore (40). The second COS-B Catalogue (2CG), which will be publi-
shed shortly by the Caravane Collaboration, has been included by W.
Hermsen in his Ph.D. Thesis at the University of Leiden (41). Although
evidently not yet representative of the final results of the COS-B mis-
sion (a more advanced edition is currently under preparation), the 2CG
Catalogue represents most of the data acquired during the first three
years of COS-B operation and it is the result of a systematic analysis
covering the entire galactic plane. The data used were obtained in 32
separate observation periods corresponding each to about one moth poin-
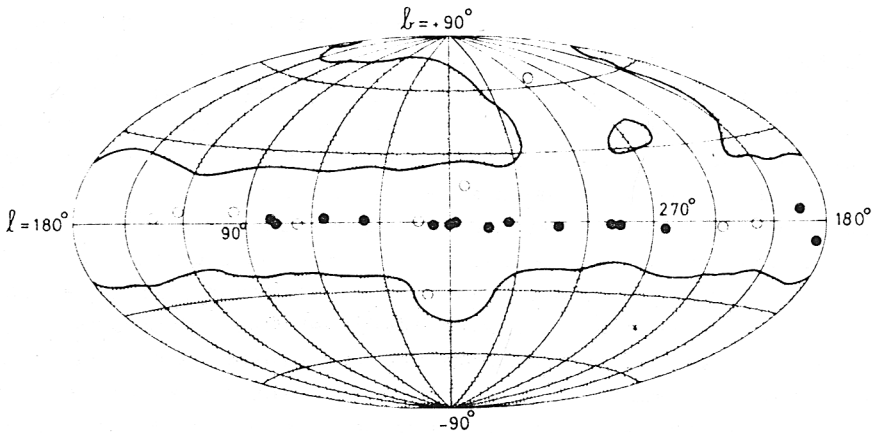
Fig. 8. Region of the sky searched for gamma-ray sources (unshaded) and
      sources detected above 100 MeV by spatial analysis. The closed
      circles denote sources with measured flux $\geqslant 1.3 \times 10^{-6}$ photons/
      /cm^2 s. Open circles denote sources below this threshold.

ting to a given target (Fig. 8).
For each observation a useful field of view inside 20° from the point-
ing axis was retained. For overlapping regions the data were merged;
in these cases information on possible time variability was lost.
A gamma-ray source is defined as a significant excess above the local
background which has a spatial distribution consistent with the instru-
ment intrinsic point-spread function. This function corresponds to the
distribution of the photon arrival directions expected from a point
source in the sky as determined by preflight calibration of the telesco
pe at accelerators and confirmed by the actual flight data for the
strong source PSR 0833-45. It must be stressed that a truly point-like
object and a feature extending to about 1° are not distinguished; for
this reason the meaning of a "Gamma-ray discrete source" is in princi-
ple different from the current meaning associated to a source in an X-
-ray catalogue.

Explication of Notes to the 2CG Catalogue

1. Expressed in Units of Standard deviations of local background (inclu
   ded contribution from the excess counts).
2. Expressed in MeV.
3. In degrees.
4. In units of 10^{-6} (photons/$\text{cm}^2 \cdot$s), for $E \geqslant 100$ MeV.
5. Intensity ($E \geqslant 300$ MeV)/intensity ($E \geqslant 100$ MeV); both intensities are
   calculated assuming an Energy spectrum E^{-2}.

(For note expl. see foll. page)

The 2CG Catalogue of Gamma-Ray sources (ref. 41)

Source name	Observation periods.	(1) Signif- icance	(2) Energy thresh.	(3) Position ℓ b	(3) Error radius.	(4) Flux	(5) Spectral parameters	Identification. Comments
2CG006-00	2,18,25	10.2	300	6.7 -0.5	1.0	2.4	0.39±0.08	
2CG010-31	30	5.7	100	10.5 -31.5	1.5	1.2	-	
2CG013+00	2,8,18,25	5.3	300	13.7 0.6	1.0	1.0	0.68±0.14	
2CG036+01	9,25,26	4.9	300	36.5 1.5	1.0	1.9	0.27±0.07	
2CG054+01	9,25,26	5.3	100	54.2 1.7	1.0	1.3	0.20±0.09	
2CG065+00	4,9,22,26	5.5	100	65.7 0.0	0.8	1.2	0.24±0.09	
2CG075+00	4,16,22,26,36	5.8	100	75.0 0.0	1.0	1.3	-	could be an
2CG078+01	4,16,22,26,36	11.9	100	78.0 1.5	1.0	2.5	-	extended feature
2CG095+04	4,16,22	4.9	150	95.5 4.2	1.5	1.1	-	
2CG121+04	11,16,28	4.9	100	121.0 4.0	1.0	1.0	0.43±0.12	
2CG135+01	11,16,28	4.9	100	135.0 1.5	1.0	1.0	0.31±0.10	GT0236+610?
2CG184-05	1,14,17,29	20.6	100	184.5 -5.8	0.4	3.7	0.18±0.04	PSR0531+21
2CG195+04	1,14,29	27.1	100	195.1 4.5	0.4	4.8	0.33±0.04	
2CG218-00	14,18,21	6.2	100	218.5 -0.5	1.3	1.0	0.20±0.08	
2CG235-01	19,21	5.0	150	235.5 -1.0	1.5	1.0	-	
2CG263-02	3,5,12,21	35.7	100	263.6 -2.5	0.3	13.2	0.36±0.02	PSR0833-45
2CG284-00	5	6.5	100	284.3 -0.5	1.0	2.7	-	could be an
2CG288-00	5	4.8	100	288.3 -0.7	1.3	1.6	-	extended feature
2CG289+64	10,32	6.5	100	289.3 64.6	0.8	0.6	0.15±0.07	3C 273
2CG311-01	5,7	5.6	150	311.5 -1.3	1.0	2.1	-	
2CG333+01	7,13,24	5.4	300	333.5 1.0	1.0	3.8	-	
2CG342-02	2,7,13,18,24	8.9	300	342.9 -2.5	1.0	2.0	0.36±0.09	
2CG353+16	2,13,18,24	5.1	100	353.3 16.0	1.5	1.1	0.24±0.09	ρ-Oph dark cloud?
2CG356+00	13	5.3	300	356.5 0.3	1.0	2.6	0.46±0.12	may be variable
2CG359-00	2,18,24	6.3	300	359.5 -0.7	2.0	1.8	-	

The 2CG Catalogue

- As for the first source catalogue, the source name is expressed by
  the symbol CG followed by the truncated value in degrees of the galac
  tic longitude and of the galactic latitude.

- Because of the complex structure of the galactic gamma-ray emission
  and its variation with ℓ and b, it is difficult to maintain a suffi-
  ciently uniform source visibility throughout the Galaxy. To improve
  uniformity only events with energy greater than 100 MeV have been ac-
  cepted, their direction of arrival being sorted in $0.5° \times 0.5°$ bins;
  moreover the exposure in regions of high sky background (e.g. Galac-
  tic Center region) has been increased.

- Statistical significance of the associated count excess at the level
  of at least 4.75 σ has been required; this procedure together with
  the fact that sources which have been at least twice in the field of
  view have been seen in each observation, assures that the number of
  spurious detectionsis insignificant. The one exception of non repea-
  ted observation (2CG356+00) is a possible example of variability.

- Some of the sources listed in the first CG or in lists previously
  published are not present in the 2CG Catalogue; the reason can be either
  because of the more extended data set the source has been better ana-
  lysed and it has revealed itself as an extended feature, or because
  it has too soft an energy spectrum to show up above threshold at 100
  MeV.

- The direction ℓ and b listed corresponds to the peak direction of
  the correlated spread function. The error radius (90% confidence le-
  vel) has been estimated from simulations.

- To derive an integral flux above 100 MeV, a power law E^{-2} has been
  adopted for the differential energy spectral shape; this is certainly
  not correct in most cases, but sufficient for a 30% approximation.

- The spectral parameter indicated in the Catalogue list gives a rough
  indication of the hardness of the spectrum above 100 MeV; the spread
  in the value for the different sources indicates significant diffe-
  rences between the spectra.

- The 2CG Catalogue, although representative of the general galactic
  picture, is certainly not complete; this fact has to be taken in mind
  in making extrapolations and in deriving conclusions.

3. GAMMA-RAY SOURCE IDENTIFICATION

I - The Crab and Vela Pulsars

Sure identification of CG sources is established only for 2CG263-02 and
2CG185-04 corresponding to PRS0833-45 (the Vela Pulsar) and to
PRS0531+21 (the Crab Pulsar) respectively; the timing signature gives
a proof of the identification beyond any doubt. The two sources repre-
sent the most intense and the third most intense source in the gamma-

-ray sky. They are extensively described in the literature; for COS-B data see ref. 42-44.

Table 3 shows the relevant parameters for the two sources:

<p align="center">Table 3</p>

CG Source	PSR	Distance	Age	$L_\gamma^{(+)}$ erg/s	$\dot{E}$ erg/s	$L_\gamma / \dot{E}$
2CG263-02	PSR0833-45	500 pc	10^4 yr	4.0×10^{34}	7.0×10^{36}	5.7×10^{-3}
2CG185-04	PSR0531+21	2000 pc	10^3 yr	1.9×10^{35}	7.8×10^{38}	2.5×10^{-4}

(+) A beaming factor 0.184 is included. $L_\gamma = 0.184 \cdot \text{Flux} \cdot E_\gamma \cdot 4\pi \, d^2$.

II - The Quasar 3C273

The location at high galactic latitude, in a region of low and rather uniform background, makes possible the identification of the source 2CG289+64 with the Quasar 3C273 on the basis of a positional coinciden ce. The source has been seen in two observation periods (39-45) and the probability of a chance coincidence of the gamma-ray source with 3C273 is estimated at 10^{-3} (45) (Fig. 9). In Fig. 10 the energy spectrum obtained by COS-B is shown together with the data obtained by HEAO-1/A2 and A4.

III - The Source 2CG135+01

Fig. 11 shows the error cicle obtained by COS-B with the cross-correla-
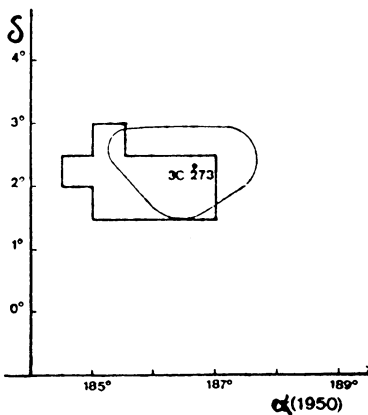
Fig. 9. COS-B observation of 2CG289+64. Thin line: 90% con fidence level contour with the likelihood method. Thick line: 6 contour with cross corr. method.
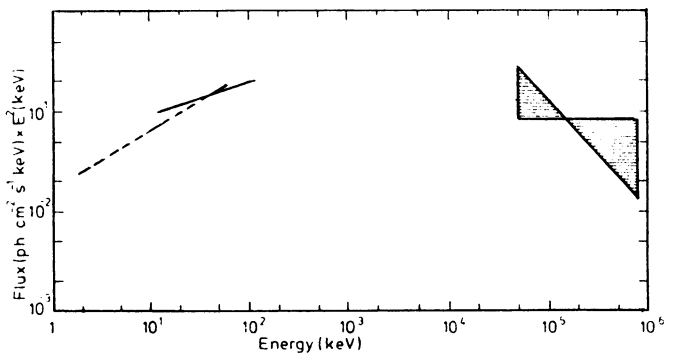
Fig.10. High energy spectrum of 3C273; dotted line: HEAO1/A2; thick line: HEAO1/A4; shaded area: COS-B.
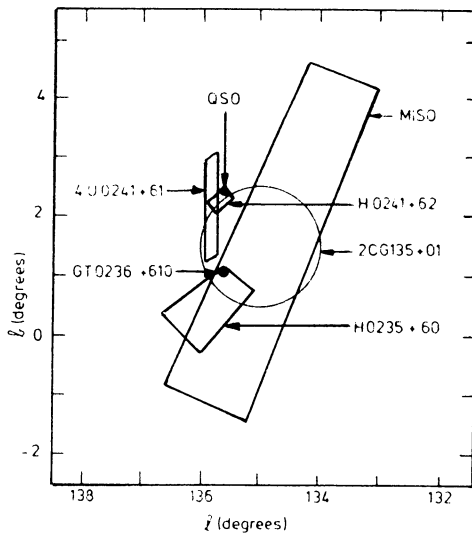
Fig. 11. Error circle for 2CG135+
+01 obtained with the crosscorre-
lation method in the COS-B data.
Indicated are also the position
and error boxes of objects identi_
fied at other w.l.
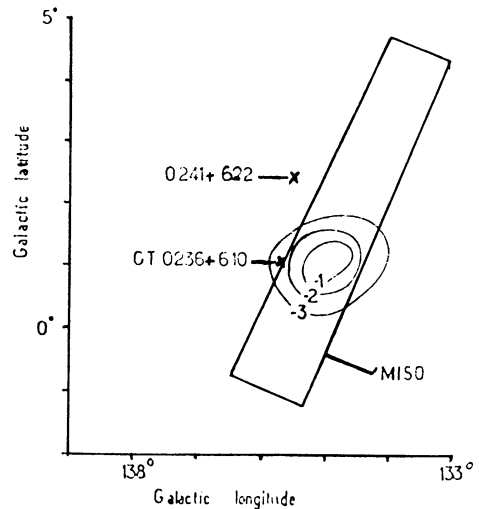
Fig. 12. Contours of constant like-
lihood for the location of a point
source of 150 to 5000 MeV in the
region of QS00241+622 and the ra-
diostar GT0236+610.

tion method for the source 2CG135+01, together with the positions of
the QSO 0241+622 and of the variable radio star GT0236+610. Fig. 12
shows the same data with the indications deriving from the likelihood
method which tests the hypothesis that the presence of the one or the
other source explain the COS-B observation best (46). This procedure
gives evidence for the identification of the gamma-ray source with the
radiostar rather than the QSO. The optical counterpart of GT0236+610
has been reported as an 11th magnitude OB$^+$ star (LSI+61°303) at 2.3Kpc
distance (47,48). A probable association with the source is represented
by the low energy gamma-ray source reported by the MiSo Group (49) at
energy above 120 KeV; recently (41) the Eistein Observatory has identi-
fied an X-ray source in the 1-3 KeV energy range, compatible with the
position of LSI+61°303.

IV - 2CG Source-Cloud Complex associations
Association between a gamma-ray source and a cloud complex, always be-
cause of positional coincidence, has been suggested for some elements
of the Catalogue of COS-B.

a) 2CG353+16 and the ρ-Oph dark cloud complex
The source lies in a region of comparatively low confusion due to back-

ground. The ρ-Oph dark cloud complex, which is at a distance of $\sim$160pc, was suggested to be detectable as a gamma-ray source above 50 MeV several years ago by Black and Fazio (50), the gamma ray flux deriving from the interaction of the cosmic radiation with the matter of the cloud. The cloud is expected to be a "passive" actor, with no indipendent compact gamma-ray emitter. To account for the gamma-emission detected by COS-B it is however necessary to speculate on the possibility of a cosmic ray flux locally higher than that at the Sun, or otherwise to some other mechanism at work to supply the missing intensity (51); on the other hand everything appears normal to other authors (52).

b) The Carina Region

W. Hermsen (41) reports the coincidence in position between 2CG284-00 and the small cluster Wd1 and of 2CG288-00 with NGC3372. Montmerle et al. (53) also suggest that the source at $\ell=288°$ and $b=0°$ should be identified with the Carina complex; in this case the source should be at $\sim$ 2.7 Kpc and its gamma-ray luminosity, above 100 MeV, $\sim 2.10^{35}$ erg s^{-1}. Because of the nature of the region considered, it is difficult to identify straigthforward and simple mechanisms for the gamma-ray source. It is interesting the model proposed in (53) involving the interaction of locally injected cosmic rays with the matter of the molecular cloud.

c) The Orion Cloud complex

To complete the list of gamma-ray localized emission possibly associated with molecular cloud complexes, we report the finding by COS-B of strong emission above 100 MeV from two centroids roughly located at $\ell==209°$, $b=-20°$ and $\ell=206°$, $b=-16°$, coinciding with the dark clouds L1630 and L1641 (54). The observation represents the first extended, and yet localized "source" of gamma-rays, coinciding with a known astronomical object. For its peculiarity of not being compatible with the COS-B point spread function corresponding to a point-like source, the Orion gamma source will not be listed in the COS-B Catalogue.

3.1. The localized sources as a "class" of objects

What preceeds, shows that only a small fraction of the gamma-ray sources of the Cos-B Catalogue can be associated with an astronomical object known at other wavelengths. In reality this is possible with certainty with only the two Pulsars (Crab and Vela), while for the other few cases the identification, if real, is not unambiguously sustained by the positional coincidence.
Searches for counterparts have been attempted far various classes of astronomical entities, but up to now with little success, mainly because of the large error box associated with the CG sources (typically 3 to 4 square degrees, with few examples down to half a square degree). In these conditions, if no timing signature is present, only a "class"

association on a purely statistical basis is possible, with the caution
that in any case the significance of the result is essentially specula-
tive. We recall here, as examples, the search for optical counterparts
by Van den Bergh (55), who reached the conclusion that statistically a
relevant fraction of the CG sources is associated with young SNR or
with compact objects related to these remnants. Montmerle (56) identi-
fies a possible association, for about half of the CG sources, with
"SNOBs" (=Supernova + OB association). A search for very high energy
(100 - 1000 GeV) gamma-ray emission from a sample of the 100 MeV sour-
ces has been made by Helmken and Weekes (57), with only upper limits
as result.

The Caravane Collaboration itself is presently carrying on a programme
for the systematic search in the error box of selected sources, of coun
terparts in the X-ray KeV region with the Satellite Einstein and for
the presence of not yet discovered Radio Pulsars in a "very deep" sur-
vey covering the period interval from about 10 msec to the order of se-
conds; this part of the programme is made in collaboration with R.N.
Manchester at the Parks and Tidbinbilla Radiotelescopes and with R. I-
saacman and D. Ferguson at Arecibo.

3.2. "2CG Source" average characteristics

A qualitative inspection of Fig. 8 shows immediately the ga-
lactic nature of the great majority of the sources of the 2CG catalo-
gue. In fact, leaving out the three high latitude entries (2CG289+64,
supposedly extragalactic and associated with the QSO 3C273, 2CG353+16
with the proposed association to the nearby ρ -Oph dark cloud and the
still unidentified 2CG010-31), the remainig 22 objects appear rather
uniformly aligned along the galactic equator, region which has been
extensively and uniformly covered by COS-B for the data concerning the
construction of the catalogue.

The (b,ℓ) distribution of the sources shows the well known "hat brim"
effect typical of the relevant galactic tracers (Table 4).

We can divide the galactic longitude in two regions: a first one corre-
sponding essentially to the outer galaxy ($60° < \ell < 300°$) and the other

Table   4

ℓ	$180°-90°$	$90°-30°$	$30°-330°$	$330°-270°$	$270°-180°$
b	$+3°.2$	$+0°.9$	$-0°.3$	$-0°.8$	$-1°.1$
No.of sources	3	5	6	3	5

corresponding to the inner galaxy, inside the solar circle ($60° > \ell > 300°$).

3.2.1. The outer Galaxy

13 of the low latitude 2CG sources belong to this region. The LogN-LogS distribution (Fig. 13) is in reasonable agreement with the assumption of a thin disk uniformly filled with sources ($N \sim S^{-1}$). The absence of a flattening down to the limit of detectability at $\sim 10^{-6}$ ph/cm^2 s (above 100 MeV) favors the assumption of an unbiased collection of data down to the visibility limit: this is reasonable taking into account the comparable level of the continuum background all over this region. By considering the source spread around the galactic equatorial plane we obtain:

$|b| = 2.1°$ around b=0°

$|b| = 1.4°$ around the slanting plane defined by the "hat brim" figure. For a population with a scale height of 50 pc (we take this value as a reference not as an absolute indication) we would have for the outer galaxy sources a characteristic distance of $d \sim 1.4$ Kpc with reference to the equatorial plane b=0°, turning to $d \sim 2$ Kpc if the "hat brim" figure is taken as reference. Considering the average flux of 2.8 10^{-6} ph/cm^2 s above 100 MeV and an average photon energy $\overline{E}$ = 250 MeV, we derive a characteristic luminosity L_γ = 2.5 10^{35} ergs/s (ref. b=0°) or L_γ =5.3 10^{35} ergs/s (ref. "hat brim").

Table 5 shows a comparison between the characteristic values deduced and those of the sources identified in the sample (2CG184-05 and 2CG263-02) or for which an identification is suggested (2CG288-00). No beaming factor is introduced.

Table 5

	characteristic values b=0°	"hat brim"	2CG184-05	2CG263-02	2CG288-00
d(pc)	1400	2000	2000	500	2700
L (ergs/s) (E_γ >100 MeV)	2.5×10^{35}	5.3×10^{35}	1×10^{36}	2×10^{35}	2×10^{35}

3.2.2. The inner Galaxy

The region contains 9 sources of the 2CG catalogue. The average $|b|$ for this sample is 1° with no significant difference between the reference to b=0° or to the "hat brim" figure of the galactic equatorial plane.

The characteristic distance is ~ 3 Kpc, always on the assumption of a scale height of 50 pc above the plane. The characteristic luminosity
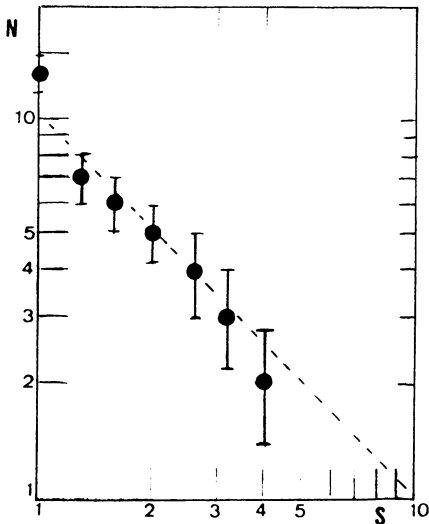
FIG.13

FIG. 14

LogN-LogS distribution for the
2CG sources in the outer galaxy
$(60° < \ell < 300°)$. S is in units
of 10^{-6} ph/cm^2 s.
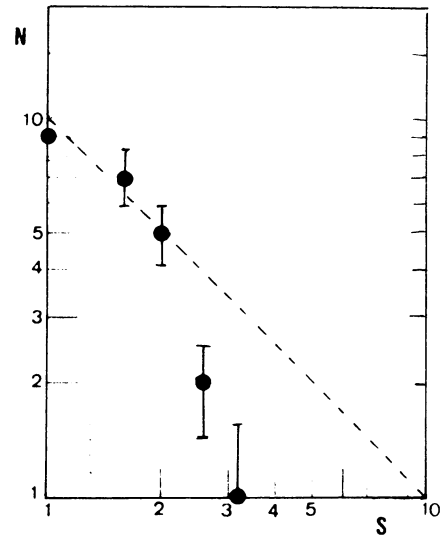
LogN-LogS distribution for the
2CG sources in the inner galaxy
$(60° > \ell > 300°)$. S is in units of
10^{-6} ph/cm^2 s.

deduced from the average flux turns out to be $L_\gamma = 9.10^{35}$ ergs/s. This
value seems to be higher than that deduced for the outer galaxy; on
the other hand the higher background level for the central region has
apparently raised the minimum detectable flux value for a discrete
source to $1.3 \ 10^{-6}$ ph/cm^2 s (for $E_\gamma > 100$ MeV) instead of $1 \ 10^{-6}$ ph/cm^2 s
for which, in the outer region, the sample appears to be unbiased. When
this is taken into account and the comparison is made for similar con-
ditions (namely sources with flux higher than $1.3 \ 10^{-6}$ ph/cm^2 s), an
identical value for the luminosity is obtained in the case of disper-
sion around the "hat brim" figure.
Considering the distribution in ℓ close to the galactic centre, within
about 30°, Hermsen (41) derives a maximum distance of ~ 7 Kpc for the
individual entries of the 2CG catalogue for the inner galaxy.
Fig. 14 shows the LogN-LogS graph for the inner galaxy sources; the di_
stribution seems difficult to be reconciled with a uniform density in
the disk and best fitted by a law $S^{-\alpha}$ with α much higher than 1. On the
other hand we must take into account the very limited statistics we are
relying upon; in fact it can be seen that all the discrepancy from the
S^{-1} law would disappear should one or two additional sources be present
with $S > 5 \ 10^{-6}$ ph/cm^2 s.

For considerations on the LogN-LogS graph for the COS-B galactic gamma-
ray sources see also (58).

3.3. Nature of the galactic gamma-ray sources: discussion

The population of gamma-ray sources in the inner and outer
galaxy appears to be the same with a luminosity $L_\gamma = 10^{35} - 10^{36}$ erg/s
(for $E_\gamma > 100$ Mev). The dynamic range of COS-B for the visibility
(somewhat less than a decade around the Crab source value) limits the
maximum distance to less than 7 Kpc towards the galactic centre while
presumably all of the outer galaxy is reachable.
The scale height is compatible with 50 pc, which is typical of various
galactic populations.
Table 6 lists the average characteristics of the 2CG sources in a simi-
lar way as presented by Hermsen in his thesis (41).

Table 6

angular size	$(1^\circ - 2^\circ)$
intensity ($>$100 MeV)	$(1 - 5)\ 10^{-6}$ ph/cm^2 s
energy flux ($>$100 MeV)	$(0.4 - 2)\ 10^{-12}$ W/m^2
energy spectrum	diverse; average intensity ratio consistent with E^{-2} spectrum
time variability	not excluded
characteristic distance	2 Kpc (outer Galaxy)
	3 Kpc (inner Galaxy)
X-ray luminosity (+)	$< 0.1\ L_\gamma$
Radio luminosity (+)	$<< L_\gamma$

(+) By integrating over the conventional energy interval

A hint on the nature of the 2CG sources is given by the few identified
cases:

a) Compact objects, e.g. pulsars, as suggested by the identification
   of PSR 0531+21 and PSR 0833-45. Although no other association of
   the sources with radio pulsars has been found up to now, the attri-
   bution of an important role to this class of objects is reasonable:
   the energetics involved and the scale height for young pulsars is
   coherent; the available radio pulsar surveys cannot be considered
   sufficient for an exhaustive comparison and it is necessary to wait
   for the results of the specific search which is being carried out
   at Arecibo and Parkes in the 2CG error boxes.
b) Molecular cloud complexes are reasonable candidates. Few intere-
   sting possible associations have been suggested.
c) A variety of degenerate objects going from neutron stars to black

holes can be called in. To these models the only limit is the lack
of fantasy.

3.4. Contribution of discrete sources to the total galactic emission

With the increased angular resolution and the larger data ba
se going from OSO-3 to SAS-2 to COS-B, the picture of the gamma-ray
sky has acquired numerous details. The total luminosity has been sugge-
sted to be 5 10^{38} ergs/s.

The original OSO-3 picture, dominated by a diffuse smooth emission re-
gion along the galactic plane, has acquired some structure with SAS-2,
while COS-B has definitely revealed a highly structured panorama. The
localized sources, absent for OSO-3 and a minority component for SAS-2,
are now dominating the picture given by COS-B, no matter what they re-
present, compact objects or features with angular dimension of $1°$ or so.
A quantitative estimate of their percentual contribution to the total
galactic emission has been attempted by several autnors: Bignami et al.
(59), Salvati et al. (60) and Hermsen (41) give a lower limit of 40-50%
but the contribution can be as high as to account for almost all the
galactic emission. A somewhat lower value, around 30%, is quoted by
Wolfendale at this Symposium.

The remaining galactic flux (besides that due to the localized sources)
can be accounted for by the interaction of the cosmic radiation with
the diffuse interstellar matter or the matter present in large concen-
trated structures (ϕ_γ = 2-3 10^{-25} ph/s H_{atom}, for E > 100 MeV) and by
low luminosity sources (10^{33} - 10^{34} erg /s), unable to show up indivi-
dually but adding together to simulate a diffuse emission. Salvati et
al. (60) suggest for this component the radio pulsars with age greater
than 10^5 years   accounting for $\sim 25\%$ of the total galactic emission abo-
ve 100 MeV, the remaining 75% being attributed for 25% to the truly dif
fuse processes involving the cosmic rays and the I.M. and for 50% to
the discrete high luminosity sources of the category listed in the 2CG
catalogue.

3.5. The extragalactic sky

The data analyzed up to now by the COS-B experimenters refer
to the region shown in Fig. 15 (61). With the exception of the identi-
fication of 2CG289+64 with the QSO 3C273, no positive observation of
extra-galactic localized sources has been made. Pollock et al. (61)
list upper limit values for the emission, above 50 and 150 Mev, from a
series of peculiar objects including Seyfert galaxies with an
addition of galaxies identified through their X-ray emission, quasars
arbitrarily selected with visual magnitude m_v < 16.5, BL Lac objects,
assorted active galaxies including N galaxies and other emission line
galaxies that are known as X-ray sources and some galaxies in the
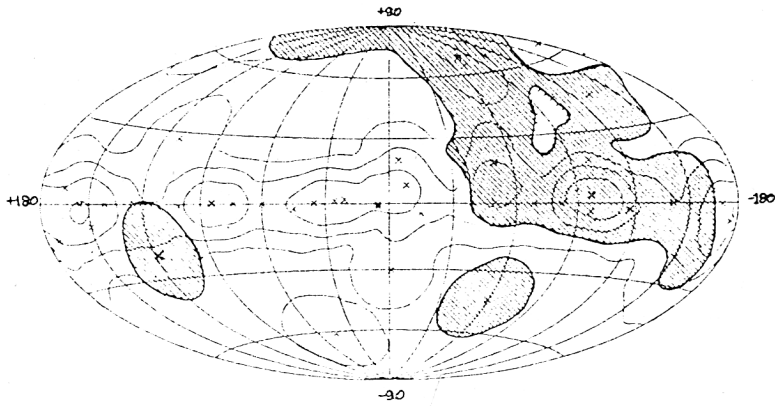
Fig. 15. Region of the sky used for the extragalactic search.

Local Group. The upper limits for the flux above 50 MeV range from 1 to 5 times 10^{-6} ph/cm^2 s confirming the conclusions obtained by SAS-2 (27) that the energy spectrum measured at X-ray energies does not extrapolate directly to gamma-rays but bends substantially much earlier.

REFERENCES

1. Hayakawa, S., 1952, Progr. Theor. Phys., $\underline{8}$, 571.
2. Hutchinson, G.W., 1952, Phil. Mag., $\underline{43}$, 847.
3. Morrison, P., 1958, Il Nuovo Cimento, $\underline{7}$, 858.
4. Frye Jr., G.M., et al., 1971, Nature, $\underline{231}$, 372.
5. Leray, J.P., et al., 1972, Astron. Astrophys., $\underline{216}$, 443.
6. Browning, R., Ramsden, D., Wright, P.J., 1972, Nature Phys. Science, $\underline{235}$, 128.
7. Parlier, B., et al., 1973, Nature Phys. Science , $\underline{242}$, 117.
8. Dahlbacka, G.H., Freier, P.S., Waddington, C.J., 1973, Ap. J., $\underline{180}$, 371.
9. Kraushaar, W.L., et al., 1965, Ap. J., $\underline{141}$, 841.
10. Kraushaar, W.L., et al., 1972, Ap. J., $\underline{177}$, 341.
11. Fichtel, C.E., et al., 1975, Ap. J., $\underline{198}$, 163.
12. Kniffen, D.A., Hartman, R.C., Thompson, D.J., Fichtel, C.E., 1973, Ap. J., (Letters), $\underline{186}$, L 105.
13. Fichtel, C.E., et al., 1978, NASA-GSFC Tech. Memorandum 79650.
14. Hartman, R.C., et al., 1979, Ap. J., $\underline{230}$, 597.
15. Fichtel, C.E., et al., 1977, Proc. 12th Eslab Symp.-ESA-SP-124, 191.
16. Fichtel, C.E., Simpson, G.A., Thompson, D.J., 1978, Ap. J., $\underline{222}$, 833.
17. Thompson, D.J., Fichtel, C.E., Hartman, R.C., Kniffen, D.A., Lamb, R.C., 1977, Ap. J., $\underline{213}$, 252.
18. Masnou, J.L., et al., 1977, Proc. 12th ESLAB Symp.-ESA-SP-124, 33.
19. Lamb, R.C., Fichtel, C.E., Hartman,R.C., Kniffen, D.A., Thompson, D.J., 1977, Ap. J., (Letters), $\underline{212}$, L 63.
20. Bennett,K., et al., 1977, Astron. Astrophys. $\underline{59}$, 273.
21. Ögelman, H.B., Fichtel, C.E., Kniffen, D.A., Thompson, D.J., 1976, Ap. J., $\underline{209}$, 584.
22. Manchester, R.N., 1980, private communication.
23. Kniffen, D.A., Fichtel, C.E., Thompson, D.J., 1977, Ap. J., $\underline{215}$, 765.
24. Fichtel, C.E., et al., 1977, Ap. J., (Letters) $\underline{217}$, L 9.
25. Fichtel, C.E., et al., 1977, Proc. 12th ESLAB Symp.-ESA-SP-124, 191.
26. Fichtel, C.E., Simpson, G.A., Thompson, D.J., 1978, Ap. J., $\underline{222}$, 833.
27. Bignami, G.F., Fichtel, C.E., Hartman, R.C., Thompson, D.J., 1979, Ap. J., $\underline{232}$, 649.
28. Scarsi, L., et al., 1977, Proc. 12th ESLAB Symp.-ESA-SP-124, 3.
29. Mayer-Hasselwander H.A., et al., 1979, Annals New York Ac. Sciences, $\underline{336}$, 211.

30. Strong, A.W., Worral, T.M., 1976, J. Phys. A. Math. Ge., 9, 823.
31. Black, J.H., Fazio, G.G., 1973, Ap. J., 185, L7.
32. Puget, J.L., Ryter, C., Serra, G., Bignami, G.F., 1976, Astron. Astrophys., 50, 247.
33. Lebrun, F., Paul, J.A., 1978, Astron. Astrophys., 65, 187.
34. Bignami, G.F., Morfill, G.E., 1980, Astron. Astrophys., 80, 1.
35. Lindblad, P.O., Grape, K., Sandqvist, A., Shober, J., 1973, Astron. Astrophys., 24, 309.
36. Rossano, G.S., 1978, Astron. J., 83, 241.
37. Caraveo, P., et al. (for the Caravane Collaboration), 1980, in preparation.
38. Hermsen, W., et al., 1977, Nature, 269, 494.
39. Swanenburg, B.N., et al., 1978, Nature, 275, 298.
40. Wills, R.D., et al., 1980, Advances in Space Expl. Vol. 7 (Pergamon Press).
41. Hermsen, W., 1980, Thesis University of Leiden.
42. Bennett, K., et al., 1977, Astron. Astrophys., 61, 279.
43. Kanbach, G., et al., 1980, Astron. Astrophys., in press.
44. Buccheri, R., et al., 1978, Astron. Astrophys. 69, 141.
45. Bignami, G.F., et al., 1980, Astron. Astrophys., in press.
46. Pollock, A.M.T., et al., 1980, Astron. Astrophys., to be published.
47. Sanduleak, N., 1978, IAU Circular n. 3170.
48. Hjellming, R., Hogg, D., Hvatum, H., Gregory, P., Taylor, R., 1978, IAU Circular N. 3180.
49. Perotti, F., et al., 1980, Ap. J., to be published.
50. Black, J.H., Fazio, G.G., 1973, Ap. J. Letters 185, L7.
51. Bignami, G.F., Morfill, G.E., 1980, Astron. Astrophys., 80, 1.
52. Wolfendale, A.W., 1980, Proc. of the IUPAP/IAU Symp. N. 94-Bologna, June 1980, in press.
53. Montmerle, T., Paul, J.A., M. Cassé, 1980, Proc. of the IUPAP/IAU Symp. N. 94-Bologna, June 1980,-in press.
54. Caraveo, P. and the Caravane Collaboration, 1980, in preparation.
55. Van den Bergh, S., 1979, Astron. J., 84, 71.
56. Montmerle, T., 1979, Ap. J., 231, 95.
57. Helmken, H.F., Weekes, T.C., 1979, Ap. J., 228, 531.
58. Bignami, G.F. and Caraveo, P.A., 1980, Ap. J., in press.
59. Bignami, G.F., Caraveo, P.A. and Maraschi, L., 1978, Astron. Astrophys., 67, 149.
60. Salvati, M., Massaro, E. and Panagia, N., 1980, Proc. of the IUPAP/IAU Symp. N. 94-Bologna, June 1980,-in press.
61. Pollock, A.M.T., et al., 1980, Astron. Astrophys., in press.